Biofilm 8 (2024) 100217



Contents lists available at ScienceDirect

Biofilm

journal homepage: www.sciencedirect.com/journal/biofilm



A cyanobacterial sigma factor F controls biofilm-promoting genes through intra- and intercellular pathways

Shiran Suban [a], Sapir Yemini [a], Anna Shor [a], Hiba Waldman Ben-Asher [a], Orly Yaron [a], Sarit Karako-Lampert [a], Eleonora Sendersky [a], Susan S. Golden [b,c], Rakefet Schwarz [a,*]

[a] The Mina and Everard Goodman Faculty of Life Sciences, Bar-Ilan University, Ramat-Gan, 5290002, Israel
[b] Division of Biological Sciences, University of California, San Diego, La Jolla, CA, 92093, USA
[c] Center for Circadian Biology, University of California, San Diego, La Jolla, CA, 92093, USA

A B S T R A C T

Cyanobacteria frequently constitute integral components of microbial communities known as phototrophic biofilms, which are widespread in various environments. Moreover, assemblages of these organisms, which serve as an expression platform, simplify harvesting the biomass, thereby holding significant industrial relevance. Previous studies of the model cyanobacterium *Synechococcus elongatus* PCC 7942 revealed that its planktonic growth habit results from a biofilm-suppression mechanism that depends on an extracellular inhibitor, an observation that opens the door to investigating cyanobacterial intercellular communication. Here, we demonstrate that the RNA polymerase sigma factor SigF1, is required for this biofilm-suppression mechanism whereas the *S. elongatus* paralog SigF2 is not involved in biofilm regulation. Comprehensive transcriptome analyses identified distinct regulons under the control of each of these sigma factors. *sigF1* inactivation substantially lowers transcription of genes that code for the primary pilus subunit and consequently prevents pilus assembly. Moreover, additional data demonstrate absence of the biofilm inhibitor from conditioned medium of the *sigF1* mutant, further validating involvement of the pilus assembly complex in secretion of the biofilm inhibitor. Consequently, expression is significantly upregulated for the *ebfG*-operon that encodes matrix components and the genes that encode the corresponding secretion system, which are repressed by the biofilm inhibitor in the wild type. Thus, this study uncovers a basic regulatory component of cyanobacterial intercellular communication, a field that is in its infancy. Elevated expression of biofilm-promoting genes in a *sigF1* mutant supports an additional layer of regulation by SigF1 that operates via an intracellular mechanism.

1. Introduction

Sigma factors play a crucial role in bacterial regulation by conferring the specificity of the RNA polymerase core complex for specific promoter sequences, facilitating transcription initiation. In heterotrophic bacteria these proteins are classified into two evolutionary and structurally unrelated families: the σ54 and the σ70 families; however, no σ54 homologs have been identified in cyanobacteria [1]. The σ70 family comprises group 1, so-called housekeeping sigma factors, as well as alternative sigma factors that dictate transcription of whole sets of genes, referred to as regulons [2,3]. Control of an entire regulon by a single sigma factor facilitates immediate response to environmental cues [4–7].

Cyanobacterial alternative sigma factors are associated with a large variety of cellular responses [1,8–12]. For example, sigma factors of the filamentous cyanobacterium *Nostoc punctiforme* promote development of motile filaments known as hormogonia [13]. In the filamentous cyanobacterium *Anabaena* sp. PCC 7120, genes *sigC*, *sigE*, and *sigG* are upregulated in heterocysts, specialized cells involved in N_2 fixation [14]. Additionally, SigF, SigG, and SigH, which belong to group 3-type σ70 factors, are required for the low-temperature growth of the unicellular marine cyanobacterium *Synechococcus* sp. PCC 7002 [15]. In *Synechocystis* sp. PCC 6803 (hereafter *Synechocystis*), mutants in *sigF* are impaired in inducing salt-stress proteins [16] and pilus assembly [17–19]. Furthermore, a *sigF*-deletion mutant of this cyanobacterium exhibits impaired vesiculation capacity compared to the wild type [20].

Recent genetic screening implied involvement of a SigF-homolog of the freshwater unicellular cyanobacterium *Synechococcus elongatus* PCC 7942 in regulation of biofilm formation [21]. Previous studies have identified a biofilm-suppression mechanism in this cyanobacterium, which relies on extracellular inhibitor(s) that repress transcription of the *ebfG*-operon. The inhibitor, which is as yet unidentified, is a small (<1 kDa) protease- and heat-resistant compound.

The *ebfG*-operon encodes four proteins that enable biofilm formation (Fig. 1; also see Refs. [22–24]). A recent study revealed cell specialization in expression of this operon – only 25 % of the cells highly express it,

* Corresponding author.
E-mail address: Rakefet.Schwarz@biu.ac.il (R. Schwarz).

https://doi.org/10.1016/j.biofilm.2024.100217
Received 8 February 2024; Received in revised form 24 July 2024; Accepted 24 July 2024
Available online 26 July 2024
2590-2075/© 2024 Published by Elsevier B.V. This is an open access article under the CC BY-NC-ND license (http://creativecommons.org/licenses/by-nc-nd/4.0/).

and yet most of the cells (>95 %) reside in the biofilm [25]. The proteins encoded by the *ebfG*-operon are secreted by a type-I like secretion system [24,26]. Moreover, EbfG1-3 are prone to form protein fibers, while EbfG4 acts as both a cell surface and a matrix protein [25]. These findings indicate that a subpopulation of cells provides "public goods" to support biofilm development by the majority of the cells.

Cumulative evidence indicates that impairment of the type IV pilus assembly complex (T4P) impairs secretion of the biofilm inhibitor thereby disrupting the suppression mechanism and leading to biofilm development (Fig. 1; also see Refs. [21,22,27,28]). Intriguingly, the RNA chaperone Hfq and a conserved cyanobacterial protein called EbsA (essential for biofilm suppression protein A) are part of the cyanobacterial T4P complex [28,29]. The glycosyl transferase Ogt, responsible for modifying the pilus subunit PilA, is required for pilus formation and biofilm-suppression [30]. However, the regulators of expression of genes related to biofilm development have not yet been identified. This study assigns a pivotal role for a sigma F homolog of *S. elongatus* in the biofilm suppression process. Furthermore, the data demonstrate the involvement of this SigF in the regulation of biofilm-promoting genes by controlling intercellular communication as well as through an intracellular mechanism.

2. Results and discussion

2.1. Inactivation of sigF1 results in biofilm development

A recent study showed that the inactivation of the gene Synpcc7942_1510, which encodes a homolog of the Sigma factor F known as SigF1, results in biofilm development in the otherwise planktonic *S. elongatus* [21]. Briefly, a pooled barcoded transposon library, RB-TnSeq, was grown, biofilms were formed, and the sequencing of the barcodes indicated the abundance of each mutant in both the biofilm and the planktonic fractions. Data analysis revealed that Synpcc7942_1510 mutants are significantly over-represented in the biofilm, indicating the potential involvement of this gene in biofilm suppression. To characterize the specific role of SigF1 in biofilm suppression, the gene was inactivated by transformation with an allele disrupted by the *Mu* transposon (Fig. 2A and Table S1). The resulting mutant, *sigF1*::Mu, was then grown separately to observe its biofilm-forming ability.

Confocal fluorescence microscopy demonstrated the presence of robust biofilms of *sigF1*::Mu (Fig. 2B). Additionally, quantification of biofilm formation was achieved by measuring the relative amount of chlorophyll in the planktonic fraction of the culture [31]. On the second day of growth, *sigF1*::Mu initiated biofilm formation, with approximately 60 % of the chlorophyll in suspended cells, in contrast to *pilB*::Tn5, which remained planktonic at this time point (Fig. 2C, day 2). By day 3, *sigF1*::Mu showed robust biofilms, with less than 5 % of the chlorophyll in suspended cells, whereas *pilB*::Tn5 initiated biofilm formation at this time point (Fig. 2C, day 3). Both mutants exhibited robust biofilms on day 6; however, significant differences were observed (percentage of chlorophyll in planktonic cells was 3.8 % ± 1.1 for *pilB*::Tn5 mutant and 1.1 % ± 0.8 for *sigF1*::Mu mutant ($p < 5\ E^{-5}$), Fig. 2C, day 6).

To validate the requirement of SigF1 for biofilm suppression and exclude potential polar effects on neighboring genes, the *sigF1* gene was introduced into a neutral site in the chromosome of *sigF1*::Mu (Table S1). The resulting strain, *sigF1*::Mu/*sigF1*, grew planktonically at all time points, confirming the role of SigF1 in suppressing biofilm formation (data shown for day 6, Fig. 2C).

S. elongatus possesses an additional SigF paralog (Fig. 2A), denoted SigF2 [32], which is homologous to SigJ of *Anabaena* sp. PCC 7120 [9,33]. SigF2 shares the R2 and R4 domains with SigF1 but lacks the R3 domain (Fig. 2A). Deletion of *sigF2* (Δ*sigF2*), however, did not affect planktonic growth (Fig. 2C, day 6). This outcome indicates that SigF2 is not involved in biofilm inhibition.

Examining the total chlorophyll accumulation up to day 6, it was found that the *sigF1*::Mu mutant had an approximate reduction of 25 % compared to the wild type, while no significant distinctions were observed between the WT, *pilB*::Tn5, and Δ*sigF2* mutants (see Fig. S1). Inactivation of the single *sigF* gene of *Synechocystis* also led to diminished chlorophyll accumulation [20].

In summary, the divergent behaviors of *sigF1*::Mu biofilm formation in contrast to the planktonic growth of Δ*sigF2*, along with the presence of the R3 domain solely in SigF1, indicate distinct cellular roles for these two sigma F factors in *S. elongatus*.

2.2. Conditioned medium from WT cultures inhibits biofilm formation by sigF1:Mu

Previous studies showed that conditioned medium (CM) from WT culture effectively inhibits biofilm formation by *pilB*::Tn5 (Fig. 3, [22,24]). Thus, *pilB*::Tn5 can recognize and react to a biofilm inhibitor produced and secreted by the WT strain even though this mutant does not auto-inhibit biofilm formation. To investigate whether *sigF1*::Mu responds to or remains unaffected by externally supplied biofilm inhibitor, we introduced this mutant into WT-CM. Similar to *pilB*::Tn5, biofilm formation by *sigF1*::Mu was entirely inhibited by WT-CM (Fig. 3) - all chlorophyll remained in the planktonic fraction when either one of the mutants was grown in CM, in stark contrast to the robust biofilms formed in fresh medium (Fig. 3). Thus, SigF1 is not necessary for the mechanism responsible for detecting or transmitting signals from the extracellular inhibitor. Likely, an as yet unknown mediator, which is present in *sigF1*::Mu as well as in *pilB*::Tn5, allows repression of the *ebfG*-operon in response to the extracellular inhibitor.

Additionally, we tested whether CM from cultures of *sigF1*::Mu inhibits biofilm formation. *pilB*::Tn5 inoculated into *sigF1*::Mu-CM formed robust biofilms, similarly to the biofilms formed in fresh medium (Fig. S2). We conclude that *sigF1*::Mu, like *pilB*::Tn5, is impaired in synthesis or secretion of the biofilm inhibitor but is capable of sensing and responding to inhibitor that is present in WT-CM.

2.3. sigF1 shares high cofitness scores with genes that encode T4P components

To gain insight into the cellular pathways that the SigF proteins of

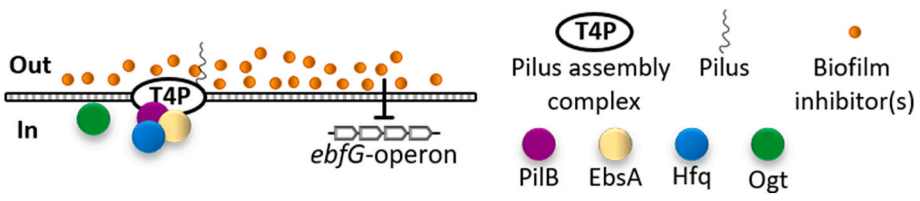


Fig. 1. Expression of genes that enable biofilm formation is governed by extracellular inhibitor(s).
PilB – assembly ATPase of the type IV pilus (T4P) assembly complex. EbsA – essential for biofilm suppression protein A. Hfq – homolog of RNA chaperone. Ogt – glycosyltransferase that glycosylates the pilus subunit PilA. The *ebfG*-operon encodes four secreted proteins that enable biofilm formation and are characterized by a double Glycine secretion motif.

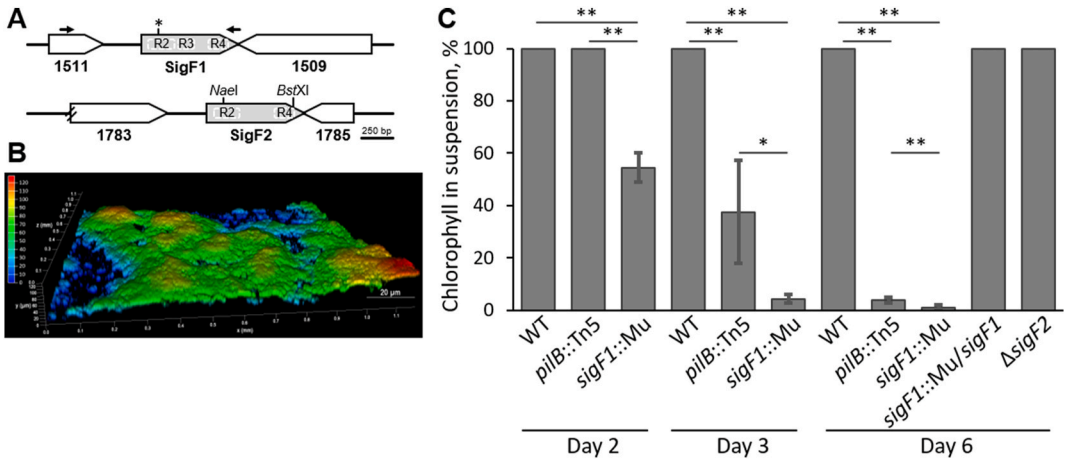


Fig. 2. SigF1 is essential for the biofilm self-suppression mechanism.
A. Genomic region of genes that encode homologs of sigmaF factors of *S. elongatus*: synpcc7942_1510 and synpcc7942_1784. R2, R3 and R4 indicate particular domains of the SigF proteins. The asterisk denotes the insertion site of the Mu transposon in *sigF1*. *Nae*I and *Bst*XI sites were used to construct the deletion mutant of *sigF2*. Arrows denote the primers used to PCR-amplify a DNA fragment for complementation. synpcc7942_1511, synpcc7942_1783 and synpcc7942_1785 encode proteins defined as hypothetical, whereas synpcc7942_1509 encodes trmU (tRNA (5-methylaminomethyl-2-thiouridylate)-methyltransferase). **B.** Image of *sigF1*::Mu biofilm obtained with confocal fluorescence microscopy. Imaging is based on autofluorescence (excitation at 630 nm and emission at 641–657 nm). The color scale represents biofilm depth. **C.** Assessment of biofilm development by measurement of the percentage of chlorophyll in suspended cells. Robust biofilm development is manifested by a low percentage of chlorophyll in the planktonic fraction (suspended cells). Strains analyzed: WT; the biofilm-forming strains in which *pilB* and *sigF1* were inactivated (*pilB*::Tn5 and *sigF1*::Mu, respectively); *sigF1*::Mu complemented with SigF1 (*sigF1*::Mu/*sigF1*) and a deletion mutant of *sigF2* (Δ*sigF2*). Data represent averages and standard deviations from 3 independent biological repetitions (with 3 technical repeats in each). Asterisks denote significance (*t*-test, two tails, two-sample assuming unequal variances. *$p < 0.001$; **$p < 5\ E^{-5}$). (For interpretation of the references to color in this figure legend, the reader is referred to the Web version of this article.)

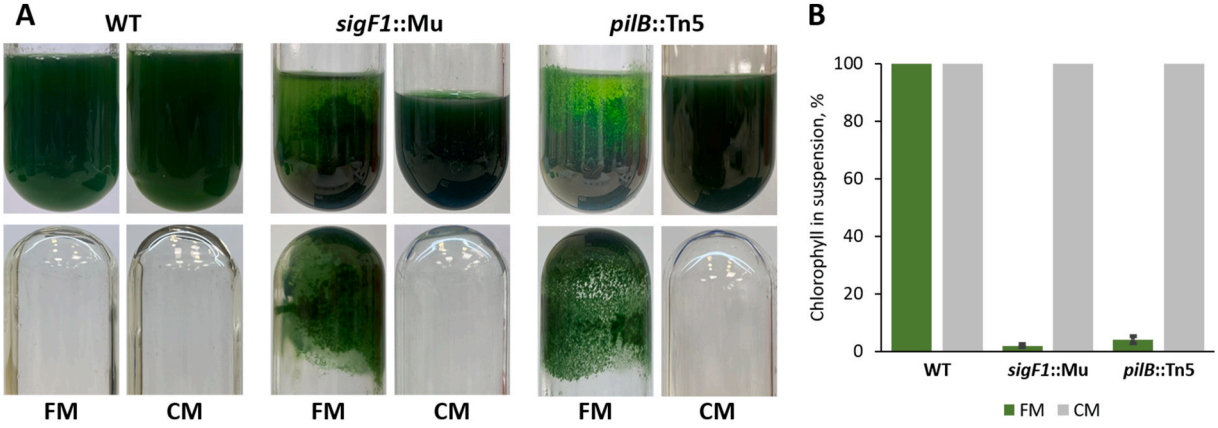


Fig. 3. Conditioned medium from WT culture inhibits biofilm formation by *sigF1*::Mu.
A. Cultures of *sigF1*::Mu and *pilB*::Tn5 in fresh medium (FM) and in WT conditioned medium (CM). Growth tubes were photographed before (upper panels) and after (lower panels) planktonic cells were decanted. In FM mutant cells adhere to the growth vessel. **B.** Percentage of chlorophyll in suspended cells served to quantify biofilm formation.

S. elongatus regulate, we examined co-fitness values, which associate the loci of an RB-TnSeq library of mutants that respond similarly under particular growth conditions [34,35]. Briefly, the RB-TnSeq library was grown under a large set of nutritional and stress conditions and the abundances of mutants, as monitored by sequencing of the barcodes, allowed determination of fitness of each mutant to a particular growth condition. Genes are defined to have strong co-fitness, and potentially act in similar pathways, if they have co-fitness scores >0.75. *sigF2* mutants do not show strong co-fitness with other genes (Table S2). Inactivation of *sigF1*, however, affected fitness similarly to inactivation of genes encoding components of T4P and the DNA competence machinery, all of which have very high co-fitness values (0.89–0.99, Table 1). Additionally, mutants in genes *ebsA* and *hfq*, which encode components of the tripartite complex with PilB and are known to be essential for biofilm suppression (Fig. 1, [28]), exhibit high co-fitness with *sigF1* mutants (Table 1). These findings strongly suggest involvement of SigF1 in cellular processes associated with the T4P complex.

2.4. Transcriptome analyses of sigF1:Mu, ΔsigF2 and pilB::Tn5

To study the role of SigF1 in transcriptional regulation, we conducted comparative analyses of the global transcriptome between the WT strain and *sigF1*::Mu mutant. *pilB*::Tn5 was also included in these analyses to help identify biofilm-related transcriptional changes. Additionally, we examined Δ*sigF2* to understand how the transcriptional space is divided between the two sigma F factors of *S. elongatus*. RNA extraction was performed at two time points: day 1, when all strains were in planktonic growth, and day 4, when both *pilB*::Tn5 and *sigF1*::Mu had developed biofilms. Venn diagrams summarize differentially expressed genes (DEGs) in the mutants relative to WT (Fold >2, adjusted

Table 1
Cofitness data for *sigF1* mutants.

Gene	Name	Description/Annotation	Cofitness
2450	*pilQ*	general secretion pathway protein D	0.99
2451	*pilO*	type IV pilus assembly protein PilO	0.99
2485	*rntB*	required for natural transformation	0.99
2486	*rntA*	required for natural transformation	0.99
0168		hypothetical protein	0.99
2071	*pilB*	ATPase	0.99
2484		hypothetical protein	0.99
1139		HmpF*	0.99
1926	*hfq*	Hfq	0.99
0862	*ebsA*	EbsA	0.99
2453	*pilM*	type IV pilus assembly protein PilM	0.99
2452	*pilN*	type IV pilus assembly protein PilN	0.99
2069	*pilC*	type IV pilus assembly protein PilC	0.99
2479	*pilA2*	PilA2	0.98
1436		hypothetical protein	0.98
1110		response regulator receiver domain	0.97
0051	*ogt*	glycosyltransferase Ogt	0.94
1935	*pilD*	prepilin peptidase	0.92
0049	*pilA1*	PilA1	0.9
1924		hypothetical protein**	0.89

Column 'Gene' describes the last four digits of full gene name (synpcc7942_XXXX). *Homolog of *Nostoc punctiforme* HmpF. **Homolog of *Synechocystis* ComFB.

p-value <0.05, Fig. 4 and Supplementary dataset 1).

Distinct regulons of SigF1 and SigF2: Transcriptome analyses of 4-day old cultures revealed substantially different regulons of SigF1 and SigF2. Only approximately 10 % of the genes up- or downregulated in *sigF1*::Mu relative to WT were shared with Δ*sigF2* (32 of 277, and 26 of 265, respectively). Notably, at this time point, SigF1 governs a larger regulon compared with SigF2 (Fig. 4 B&D; 277 vs. 37 upregulated genes and 265 vs. 43 downregulated genes). The observed differences in regulons between SigF1 and SigF2 can likely be attributed to the distinct domain compositions of these sigma factors, which may affect their promoter specificity and consequently dictate the regulation of different sets of genes. Moreover, the presence of both up- and downregulated genes in each mutant suggests that both SigF factors are involved in transcriptional repression of specific gene sets and transcription initiation of other gene sets. Transcriptional repression is most likely indirect, via transcription initiation of a repressor-encoding gene by SigF1. Upregulation of genes in *sigF1*::Mu implies that, in the absence of SigF1, another sigma factor or response regulator initiates or activates transcription of this set of genes. The putative positive transcriptional activator may drive transcription in WT cells when SigF1-modulation, possibly by posttranslational modification or anti-sigma factors, alleviates its repressive effect. Cyanobacterial anti-sigma factor candidates have been predicted based on sequence similarity to known factors from heterotrophic bacteria; however, most have not been verified experimentally [1]. A study of *Synechocystis* demonstrated that the H subunit of Mg-chelatase serves as a SigE-*anti*-sigma factor, thereby broadening the scope of proteins that may serve for sigma factor regulation [36]. An additional study implicated SapG, a SigG anti-sigma factor, in regulation of envelope stress in *Nostoc punctiforme* [37].

Several DEGs encode homologs of proteins that are involved in formation or binding of cyclic nucleotides, known regulators of biofilm development. For example, Synpcc7942_2535, which encodes a homolog of diguanylate cyclases that catalyze formation of c-di-GMP, is upregulated in *sigF1*::Mu and *pilB*::Tn5. Moreover, Synpcc7942_1716, which encodes a protein with a PAS/PAC sensor domain in addition to a diguanylate cyclase motif, is upregulated in *pilB*::Tn5 (Supplementary dataset 1, Upregulated day 4).

High transcript levels of biofilm-promoting genes in *sigF1*::Mu and *pilB*::Tn5: Transcriptome analyses revealed substantial upregulation of the *ebfG*-operon in *sigF1*::Mu. The transcript abundances of *ebfG* genes were 18–25 fold higher on day 1 and ~600–1000 fold higher on day 4 in *sigF1*::Mu compared to WT (Fig. 4 A&B and Supplementary dataset 1). Additionally, *pteB*, which encodes a cysteine peptidase that takes part in secretion and maturation of EbfG proteins [24], is upregulated approximately 270-fold in *sigF1*::Mu compared to WT (Fig. 4B).

Venn diagrams in Fig. 4B–D shows that most DEGs of *pilB*::Tn5 are encompassed within the DEGs of *sigF1*::Mu. Possibly, these shared transcriptional changes between the two biofilm-forming strains represent processes related to biofilm formation or cellular functions associated with proliferation or survival within the biofilm environment. One of these genes, synpcc7942_1132, which encodes a homolog of HlyD, a component of type I secretion systems, is upregulated in the biofilm-forming mutants (Fig. 4B). Given involvement of a type I system in secretion of the EbfG proteins [24,26] we investigated the role of *hlyD* in biofilm formation by constructing the double mutant *pilB*::Tn5/*hylD*::Mu (Table S1). This strain grew planktonically (Fig. S3); therefore, we concluded that HlyD is required for biofilm formation, most likely due to its involvement in secretion of the EbfG proteins.

A recent cryo-electron microscopy approach investigated the structure-function relationship of HlyB and HlyD of *Escherichia coli* and provided insight into translocation of the HlyA toxin [38]. The mechanism of EbfG secretion is, as yet, unknown.

Notably, on day 1, higher levels of transcripts of *ebfG*1-3 were observed in *sigF1*::Mu compared to *pilB*::Tn5 (Fig. 4A), consistent with the earlier biofilm formation manifested by *sigF1*::Mu (Fig. 2C). Additionally, a larger increase in transcript levels of the *ebfG*-operon and the biofilm-related genes *pteB* and *hlyD* was observed in *sigF1*::Mu compared to *pilB*::Tn5 (Fig. 4 A&B).

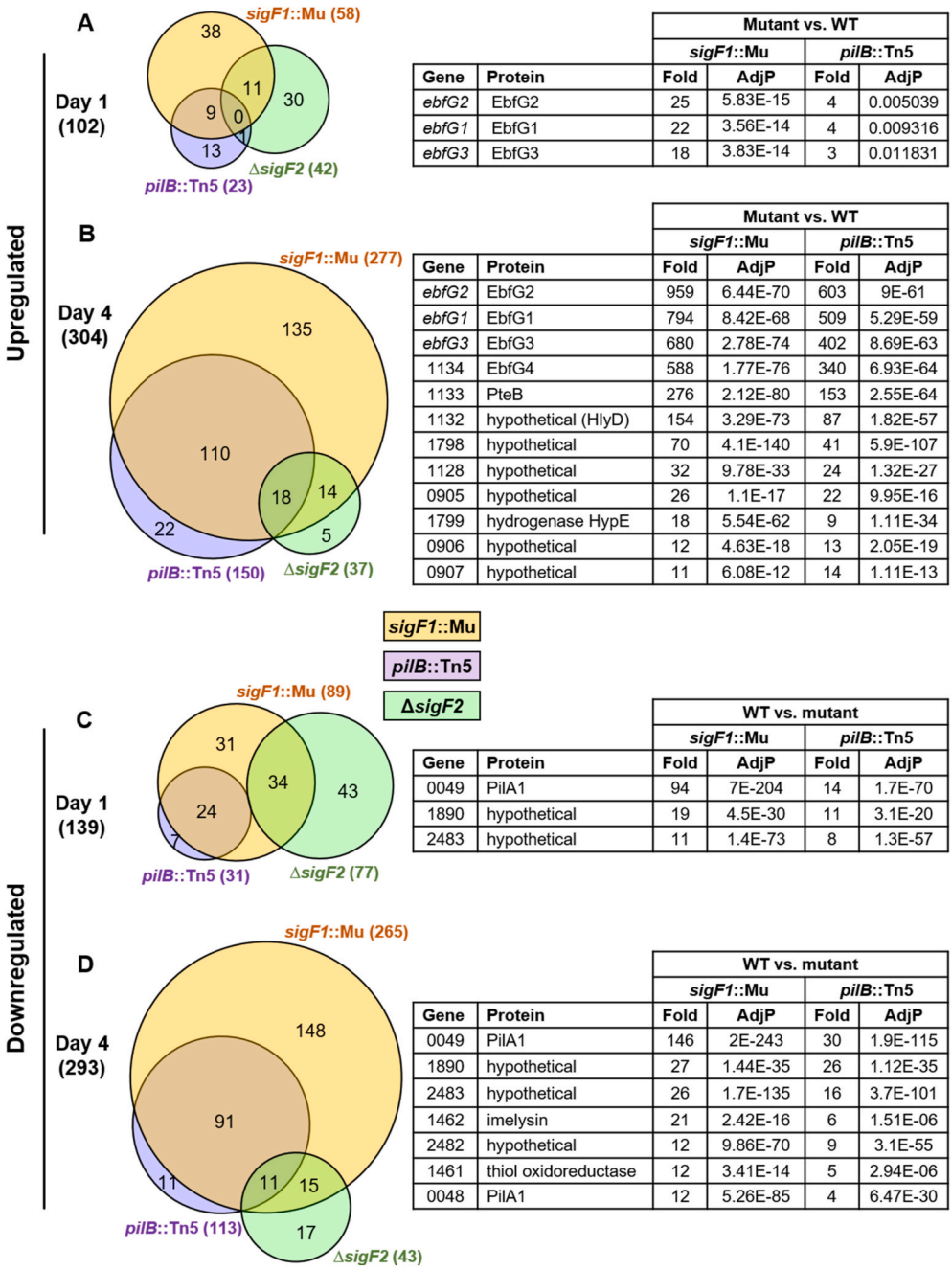
Low transcript levels of *pilA1* genes in *sigF1*::Mu: The major pilus subunit in *S. elongatus* is encoded by two adjacent genes, synpcc7942_0049 and synpcc7942_0048 [27,30,32], both referred to as PilA1 due to their 98 % amino acid identity. The majority of *pilA1* transcripts in WT cells originate from gene synpcc7942_0049 (Fig. S4). Transcript levels of this gene are 94-fold higher on day 1 and 146-fold higher on day 4 in WT compared to *sigF1*::Mu (Fig. 4C and D; see also Supplementary dataset 1). Similar, although less pronounced, differences are observed for synpcc7942_0048 (Fig. 4D). These findings suggest that SigF1 plays a role in activating the transcription of the *pilA1* genes, which, in turn, affects the secretion of the biofilm inhibitor. Of note, SigF of *Synechocystis* has been implicated in transcription activation of *pilA1* [17,19].

Gene Synpcc7942_2482 that encodes a PilA candidate [39] is downregulated in *sigF1*::Mu and *pilB*::Tn5. Inactivation of this gene, however, resulted in planktonic growth [27] and thus, this putative pilin subunit is not required for the biofilm inhibitory mechanism. Functional redundancy may also explain the observed phenotype.

2.5. Impact of sigF1 inactivation on pili formation and DNA competence

Given that *pilA1* transcripts are substantially less abundant in *sigF1*::Mu compared to WT, we examined piliation of this mutant by transmission electron microscopy (TEM). As shown in Fig. 5, pili were not observed in most *sigF1*::Mu cells (95 % non-piliated, n = 62) in contrast to WT cells (96 % piliated, n = 45). Moreover, detached pili observed in WT cultures (Fig. 5), were not detected in *sigF1*::Mu cultures. Together, low abundance of *pilA1* transcripts in *sigF1*::Mu compared to WT (Fig. 4C&D) and absence of pili in this mutant (Fig. 5) are in-line with the high co-fitness of *sigF1* mutants with mutants in components of the T4P complex (Table 1). In contrast to *sigF1*::Mu, the majority of Δ*sigF2* cells are characterized by pili (78 % piliated, n = 50; Fig. 5), in agreement with normal transcription of the *pilA1* genes in this strain (Supplementary dataset 1).

SigF involvement in transcription regulation of *pilA* and pilus formation was demonstrated in *Synechocystis* and *Nostoc punctiforme* [13,19,20,40]. Together with current observations of impaired *pilA1* transcription and absence of pili in *sigF1*::Mu of *S. elongatus*, data suggest that SigF involvement in pilus formation is a general cyanobacterial



		Mutant vs. WT			
		sigF1::Mu		*pilB*::Tn5	
Gene	Protein	Fold	AdjP	Fold	AdjP
ebfG2	EbfG2	25	5.83E-15	4	0.005039
ebfG1	EbfG1	22	3.56E-14	4	0.009316
ebfG3	EbfG3	18	3.83E-14	3	0.011831

		Mutant vs. WT			
		sigF1::Mu		*pilB*::Tn5	
Gene	Protein	Fold	AdjP	Fold	AdjP
ebfG2	EbfG2	959	6.44E-70	603	9E-61
ebfG1	EbfG1	794	8.42E-68	509	5.29E-59
ebfG3	EbfG3	680	2.78E-74	402	8.69E-63
1134	EbfG4	588	1.77E-76	340	6.93E-64
1133	PteB	276	2.12E-80	153	2.55E-64
1132	hypothetical (HlyD)	154	3.29E-73	87	1.82E-57
1798	hypothetical	70	4.1E-140	41	5.9E-107
1128	hypothetical	32	9.78E-33	24	1.32E-27
0905	hypothetical	26	1.1E-17	22	9.95E-16
1799	hydrogenase HypE	18	5.54E-62	9	1.11E-34
0906	hypothetical	12	4.63E-18	13	2.05E-19
0907	hypothetical	11	6.08E-12	14	1.11E-13

		WT vs. mutant			
		sigF1::Mu		*pilB*::Tn5	
Gene	Protein	Fold	AdjP	Fold	AdjP
0049	PilA1	94	7E-204	14	1.7E-70
1890	hypothetical	19	4.5E-30	11	3.1E-20
2483	hypothetical	11	1.4E-73	8	1.3E-57

		WT vs. mutant			
		sigF1::Mu		*pilB*::Tn5	
Gene	Protein	Fold	AdjP	Fold	AdjP
0049	PilA1	146	2E-243	30	1.9E-115
1890	hypothetical	27	1.44E-35	26	1.12E-35
2483	hypothetical	26	1.7E-135	16	3.7E-101
1462	imelysin	21	2.42E-16	6	1.51E-06
2482	hypothetical	12	9.86E-70	9	3.1E-55
1461	thiol oxidoreductase	12	3.41E-14	5	2.94E-06
0048	PilA1	12	5.26E-85	4	6.47E-30

Fig. 4. Summary of transcriptome analyses of WT, *pilB*::Tn5, *sigF1*::Mu and Δ*sigF2*.
Venn diagrams summarize differentially expressed genes (DEGs) that were up- or downregulated in the mutants relative to WT (fold change ≥2; adjusted $p < 0.05$). Tables indicate protein-encoding genes exhibiting the highest fold change for *sigF1*::Mu compared to WT (fold change >10; adjusted $p < 0.05$), which are also differentially expressed in *pilB*::Tn5 but not in Δ*sigF2*. For complete data set see Supplementary dataset 1. **A** and **B**. Upregulated genes in mutants compared to WT in day 1 or day 4, respectively. **C** and **D**. Downregulated genes in mutants compared to WT in day 1 or day 4, respectively.

mechanism.

The T4P complex is typically associated with uptake of external DNA [32,41–45]. Furthermore, inactivation of *sigF* in *Synechocystis* abolishes DNA competence [17,18]. Comparison of DNA competence in *sigF1*::Mu and Δ*sigF2* revealed that *sigF1*::Mu is characterized by DNA competence similar to WT whereas Δ*sigF2* is non-transformable (Fig. S5), in accordance with a genetic screen for genes required for DNA competence [32]. These data, together with the TEM (Fig. 5) and the transcript analyses (Fig. 4C and D), suggest that pili comprising PilA1 are those observed in TEM images of WT and Δ*sigF2*. These pili, which are absent from *sigF1*::Mu are dispensable for DNA competence. Possibly, the *sigF1*::Mu strain assembles few, thin, or short pili that are not observed by the negative staining and TEM analysis and that are functional in DNA uptake. Additionally, a glycosyltransferase mutant of *S. elongatus*, which does not glycosylate PilA1 and the majority of its cells are non-piliated, is nevertheless transformable similar to WT [30]. *S. elongatus* possesses several alternative pilin candidate genes [27,32,39]; however, the identity of the competence pili is, as yet, unknown.

2.6. *EbfG expression examined by flow cytometry*

Following up on the transcriptome results, which indicate that SigF1 is required for *ebfG*-operon transcription upregulation, we examined expression of this operon in individual cells using reporter strains and

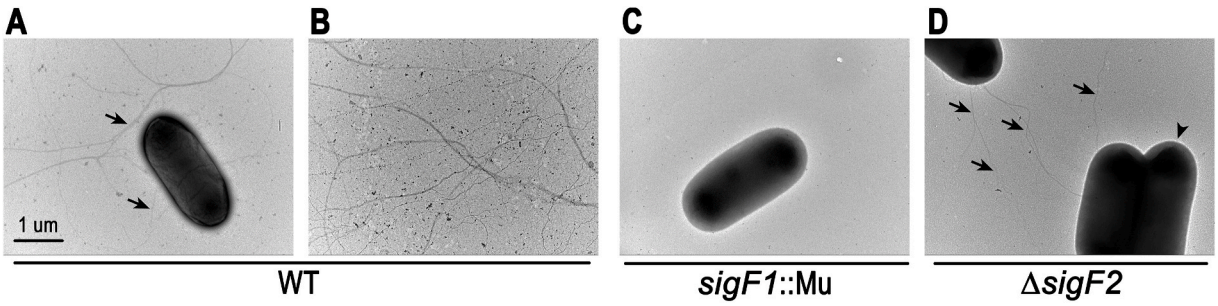


Fig. 5. Transmission electron microscopy (TEM) analyses of WT, *sigF1*::Mu and Δ*sigF2*. **A**, **C** and **D.** Cell images. **B.** Detached cell pili observed in WT culture. Arrows indicate pili whereas the arrowhead indicates a non-piliated Δ*sigF2* cell. Scale bar shown in A is relevant to all panels.

flow cytometry. The reporter construct comprises the putative promoter region of the *ebfG*-operon along with the 5' untranslated region attached to a yellow fluorescence protein (*yfp*) gene, yielding the construct P-*ebfG*::YFP. This reporter gene was inserted in a neutral site in the chromosome in WT, *pilB*::Tn5, *sigF1*::Mu and Δ*sigF2* cells, yielding their cognate reporter strains (Table S1 and [25]).

WT-reporter 2-day-old cultures served for defining YFP-positive cells for all reporter strains (dashed line in Fig. 6A, also see Fig. S6). Analysis of 2-day-old cultures, prior to biofilm development by strains capable of forming biofilms, did not exhibit significant changes between WT-, *pilB*::Tn5-and *sigF1*::Mu-reporter strains (Fig. 6B). Following biofilm development by *pilB*::Tn5-and *sigF1*::Mu-reporter cultures (day 4 and day 6), biofilm and planktonic fractions were separated and measured individually (see Methods). No significant changes were found between percentage of YFP-positive cells in the biofilm and the planktonic fractions of a particular mutant strain at a specific time point, in agreement with previous analyses of a *pilB*::Tn5-reporter [25]; therefore, data from the two fractions were analyzed collectively. Mutant reporters were distinct from the WT-reporter strain in both 4-day and 6-day old cultures (Fig. 6B).

In addition to using WT-reporter 2-day-old cultures for defining YFP-positive cells (data shown in Fig. 6B), we used 6-day-old WT-reporter cultures as a reference for YFP-positive cells in *pilB*::Tn5 and *sigF1*::Mu reporter strains at this culture stage (Fig. 6C, dashed line). This analysis revealed approximately 25 % YFP-positive cells in the *sigF1*::Mu-reporter compared to around 6 % in the *pilB*::Tn5-reporter (Fig. 6C).

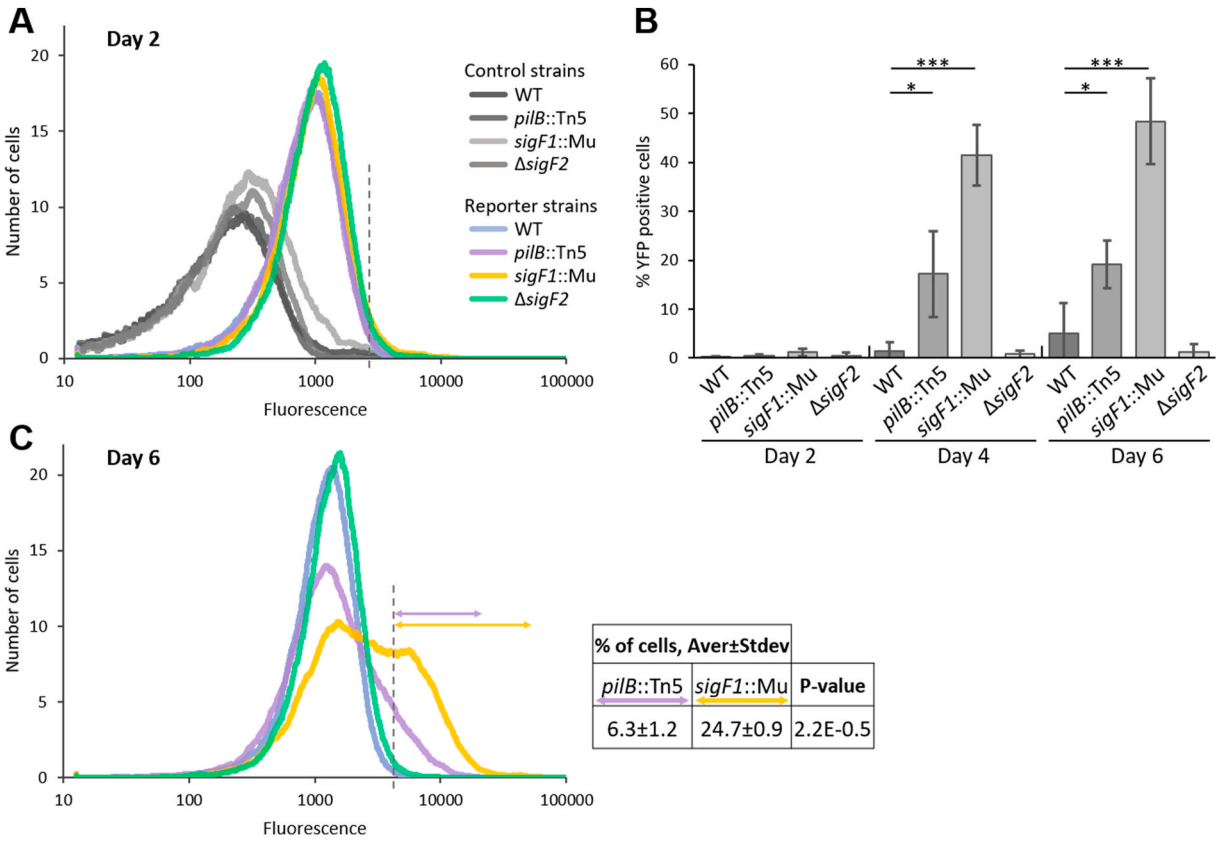


Fig. 6. Examination of expression of the *ebfG*-operon using reporter strains and flow cytometry. A and **C.** Number of cells as a function of fluorescence in WT, *pilB*::Tn5, *sigF1*::Mu and Δ*sigF2* strains bearing a reporter construct (P-ebfG::YFP). Analyses were performed on 2-day **(A)** and 6-day **(C)** old cultures. In **A** the cognate negative control strains are also included. Data shown are from a single representative experiment out of the three biological replicates. Dashed line in **A** indicates cutoff for calculating YFP positive cells (data summary in **B**). Additional cutoff (dashed line in **C**) served for calculating YFP positive mutant-reporter cells relative to 6-day old WT-reporter (see Table for averages and standard deviations from three biological replicates). **B.** Percentage of YFP-positive cells in *pilB*::Tn5, *sigF1*::Mu and Δ*sigF2* reporter cultures relative to 2-day old WT-reporter cells. Averages and standard deviations from three biological replicates are presented. Asterisks denote significant changes between WT- and mutant-reporter strains of same culture age (one-way ANOVA with Dunnett's post-hoc test. *$p < 0.05$; ***$p < 0.001$).

Notably, only a subfraction of cells in cultures of the biofilm-forming strains exhibits high expression of YFP (Fig. 6B and C), indicating cell specialization in expression of the *ebfG*-operon, in agreement with previous analyses of *pilB*::Tn5 [25]. EbfG4 is a surface and matrix-localized protein and EbfG1-3, which are prone to form amyloids, are likely to be matrix components [25]. The *sigF1*::Mu data support the premise that, through cell specialization in expression of the *ebfG*-operon, production of "public goods" by part of the population is sufficient to support biofilm development by the majority of the cells. Moreover, the higher fraction of YFP-positive cells in *sigF1*::Mu compared to *pilB*::Tn5 (Fig. 6C) is in line with the more vigorous biofilm produced by *sigF1*::Mu (Fig. 2C, day 6).

Expression of the *ebfG*-operon in Δ*sigF2* did not significantly differ from WT throughout the experiment (Fig. 6), in agreement with the transcriptome analyses (Supplementary dataset 1) and the planktonic nature of this mutant (Fig. 2).

2.7. Exoproteome analyses reveal substantially higher level of EbfG proteins in sigF1:Mu than in pilB::Tn5

Previous exoproteome analyses indicated higher amounts of EbfG proteins in CM of *pilB*::Tn5 compared to WT [27]. Elevated expression of the *ebfG*-operon and components of the type-I secretion system related to secretion of the EbfG proteins in *sigF1*::Mu compared to *pilB*::Tn5 encouraged us to compare the exoproteomes of these two mutants. Data revealed 50-3400-fold higher extracellular level of EbfG proteins in *sigF1*::Mu compared to *pilB*::Tn5 (Fig. 7A). This finding is in line with observed earlier onset of biofilm formation by *sigF1*::Mu compared to *pilB*::Tn5 (Fig. 2C).

Additionally, the exoproteome of *sigF1*::Mu is characterized by numerous proteins that are more or less abundant compared to WT (Fig. 7 B&C, also see Supplementary dataset 2). Viability assessment using SYTOX staining did not reveal significant differences between WT and *sigF1*::Mu (Fig. S7). Therefore, changes between the exoproteomes of these strains likely represent SigF1 impact on different secretion processes. Inactivation of *sigF* in *Synechocystis* also substantially affects the exoproteome [20]. Together, these observations imply that regulation of secretion processes by SigF is a common cyanobacterial mechanism.

Genes synpcc7942_0905 and synpcc7942_0906, whose transcripts are highly elevated in *sigF1*::Mu and *pilB*::Tn5 compared to WT (Fig. 4B), encode proteins of unknown function or annotation that are more abundant in the exoproteome of these mutants compared to WT (Supplementary dataset 2; independent exoproteome analysis of *pilB*::Tn5 also indicated enrichment of these proteins compared to WT [27]). Given elevated expression of these genes, and abundance of their encoded proteins in the exoproteomes of the biofilm-forming mutants, we proposed that, similarly to products of the *ebfG*-operon, these proteins may contribute to matrix formation. To test this hypothesis, a double mutant was constructed in which *pilB* was inactivated and synpcc7942_0905 and synpcc7942_0906 were deleted. This strain, however, demonstrated vigorous biofilm formation, comparable to *pilB*::Tn5 (Fig. S8), negating a need for these gene products in biofilm formation.

2.8. Summary model: SigF1 regulates biofilm formation via intra- and intercellular pathways

The data strongly support the involvement of SigF1 in the intricate regulation of genes that promote biofilm formation, acting through two distinct pathways as illustrated in Fig. 8. This alternative sigma factor plays a fundamental role in activation of *pilA1* transcription as evident by the substantially low transcript levels of the major pilin subunit (Fig. 4C&D) in *sigF1*::Mu and consequently, the major pili are absent from this mutant (Fig. 5). The T4P complex has been assigned a role in deposition of biofilm inhibitor(s) to the extracellular milieu. This activity subsequently leads to the repression of genes that promote biofilm formation (Fig. 8, top panel, thick T-bar; [21–25]). Therefore, *sigF1*-inactivation, which abrogates pili formation, alleviates a major repression pathway, most likely due to disruption of the inhibitor(s) secretion process, as supported by lack of biofilm inhibitory activity in CM from *sigF1*::Mu (Fig. S2).

Furthermore, we propose that SigF1 is involved in an additional inhibitory pathway, based on the higher expression of biofilm-promoting genes in *sigF*::Mu compared to *pilB*::Tn5 as supported by three lines of experiments: Higher levels of transcripts from the *ebfG*-operon, *pteB* and *hlyD* (Fig. 4) and elevated EbfG expression that is manifested by flow cytometry data (Fig. 6) and exoproteome analyses (Fig. 7). In *pilB*::Tn5, where the assembly ATPase of the T4P complex is inactivated, the repression exerted by the extracellular inhibitor is

A

	sigF1::Mu vs. WT		*pilB*::Tn5 vs. WT		*sigF1*::Mu vs. *pilB*::Tn5	
Protein	**Fold**	**FDR**	**Fold**	**FDR**	**Fold**	**FDR**
EbfG3	48081	3.717E-07	14	0.13	3434	2.50E-07
EbfG4	904	1.547E-05	14	0.07	65	1.70E-05
EbfG1	564	2.559E-09	8	0.01	71	3.52E-10
EbfG2	224	5.408E-09	4	0.05	56	5.86E-09

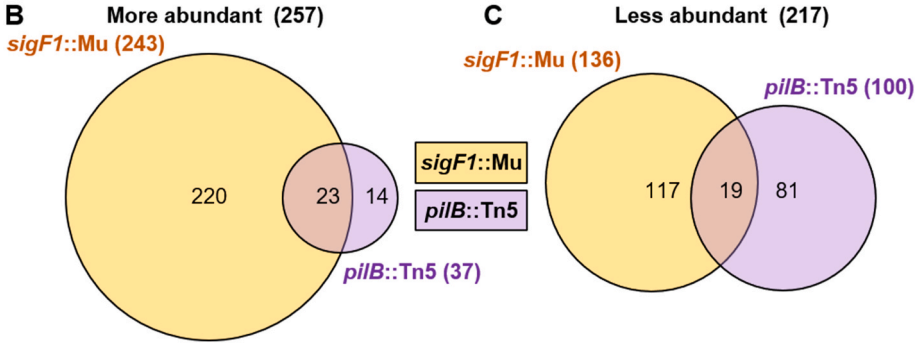


Fig. 7. Exoproteome analyses reveal substantially higher level of EbfG proteins in *sigF1*::Mu than in *pilB*::Tn5. A. Table summarizing enrichment of EbfG proteins in mutant exoproteomes. Venn diagrams summarizing more (**B**) and less (**C**) abundant proteins in the exoproteomes of *sigF1*::Mu and *pilB*::Tn5 compared to WT (fold change >2; false discovery rate (FDR) < 0.1).

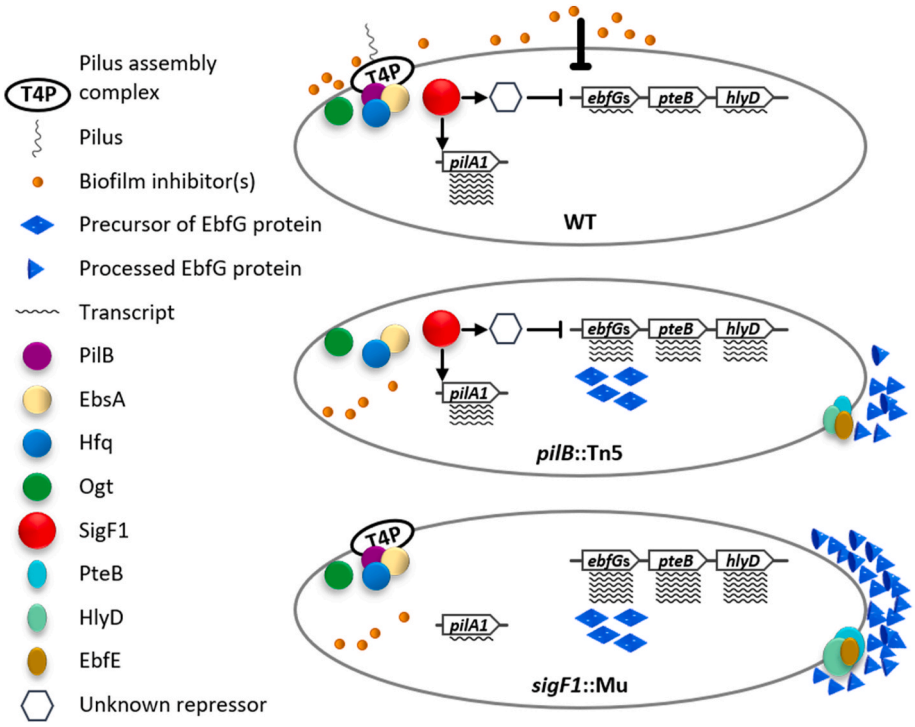


Fig. 8. Dual repression pathways by SigF1 in biofilm regulation.
SigF1 regulates transcription of biofilm-promoting genes via an intracellular mechanism (thin T-bar) as well as intercellular pathway (thick T-bar). See text for further details.

nullified; however, SigF1 also contributes to repression of EbfGs via an intracellular pathway (Fig. 8, middle panel, thin T-bar). In *sigF1*::Mu this pathway is abolished along with the intercellular pathway mediated by secreted inhibitor(s); consequently, transcription repression in *sigF1*::Mu is completely alleviated (Fig. 8). The ubiquitous presence of EbfG proteins in the *sigF1*::Mu exoproteome results from the remarkably high expression of the *ebfG*-operon and the related secretion machinery (Figs. 7 and 8).

Repression mediated by the extracellular inhibitor is the main suppression pathway of biofilm promoting components encoded by the *ebfG*-operon, *pteB* and *hlyD* (Fig. 8, thick T-bar). This conclusion is supported by planktonic growth of *sigF1*::Mu when inoculated into WT-CM (Fig. 2) – in this mutant the intracellular pathway is absent, yet operation of the extracellular pathway by supplementation of the inhibitor from WT-CM is sufficient to completely block biofilm formation. Moreover, even though the intracellular pathway is active in *pilB*:: Tn5 (Fig. 8), this mutant forms robust biofilms in fresh medium due to impairment of the extracellular pathway. Taken together, two lines of evidence support the dominance of the extracellular pathway: 1. In *pilB*:: Tn5, where the intracellular pathway is active, it is sufficient to abrogate the extracellular pathway to enable robust biofilm formation. 2. In *sigF1*::Mu, which lacks both inhibitory pathways, the inhibitor that is present in WT-CM is sufficient to completely hinder biofilm development.

Our data are consistent with the presence of two different repressors for the inter- and intracellular pathways. Response of *sigF1*::Mu to inhibitor(s) within WT-CM underscores that SigF1 involvement is not required for the perception or transduction of the inhibitory signal; the repressor that conveys this response is present in the absence of SigF1. This repressor is part of the process depicted as a thick T-bar in Fig. 8. Moreover, SigF1 likely activates another repressor (Fig. 8, hexagon) that takes part in repression of biofilm-promoting genes via the intracellular inhibitory pathway (Fig. 8, thin T-bar).

EbfG4 functions as both a cell-surface and matrix protein, and EbfG1-3 exhibit a propensity to form amyloids [25]. These observations, coupled with findings from studies in heterotrophic bacteria that attribute a role to amyloids as fundamental building blocks of the matrix [46–49], collectively support the robust matrix formation potential of *sigF1*::Mu.

Accumulation of biofilm inhibitor with culture growth and increase in cell density support a quorum-like mechanism in regulation of *S. elongatus* biofilm formation [25]. Of note, the field of cyanobacterial quorum sensing and regulation of intercellular signaling is in its infancy. Thus, this study, which assigns a role to SigF1 in intercellular communication and communal behavior, provides a step forward in elucidation of these cyanobacterial mechanisms.

The *Synechocystis sigF* mutant exhibited clumping and increased polysaccharide secretion: phenotypes that are often associated with biofilm formation. However, biofilms were not reported for this mutant [20]. It is conceivable that, under different growth conditions, this mutant could develop biofilms and, therefore, we propose that SigF involvement in biofilm regulation is likely a more widespread characteristic shared among cyanobacteria.

3. Materials and methods

3.1. Strains, culture conditions, biofilm assay, competence analysis and viability assessment

S. elongatus PCC 7942, an obligatory photoautotroph, and all derived strains were grown in mineral medium BG-11 as described [31]. Cultures were grown at 30 °C in Pyrex tubes under bubbling with air enriched with 3 % CO_2. Incandescent light was provided at flux of ~30 μmol photons m^{-2} s^{-1}. Construction of mutants and details of molecular manipulations are provided in Supplementary Table 1. CM for testing biofilm inhibiting activity was harvested from 6-day old cultures and supplemented with nutrients as described [24].

Biofilm quantification in bubbled cultures is based on chlorophyll measurement as a proxy for biomass accumulation in sessile as well as in planktonic cells and representation of the relative fraction of chlorophyll

in planktonic cells. Chlorophyll was extracted in 80 % acetone and quantified based on absorbance at 663 nm [31]. Biofilms formed under static conditions in 24-well plates at 28 °C with incandescent light illumination (30 μmol photons m^{-2} s^{-1}) were quantified after 9 days by crystal violet stanning essentially as described [50], except that crystal violet extraction was performed in 95 % ethanol and not in 30 % acetic acid. Viability assessment using SYTOX stanning was performed as described [28].

Assessment of DNA-uptake competence was performed essentially as described [51]. Exponentially growing cells were centrifuged (5000g for 8 min at room temperature), washed once with 10 mM NaCl, and re-suspended to an OD_{750} of 4.0. A shuttle vector (1000 ng) was added to 600 μl of cells, which were gently agitated overnight at 28 °C in the dark. Transformants were selected by plating on selective solid growth medium (50 μg ml^{-1} spectinomycin) supplemented with $NaHCO_3$ (5 mM) and sodium thiosulfate (0.3 %, wt./vol.). The shuttle vector replicates autonomously, thus allowing the assessment of DNA uptake without a possible impact on the efficiency of DNA integration into the chromosome.

3.2. Microscopy

To observe biofilms by fluorescence microscopy, a sterile microscope slide was inserted into a growth tube upon culture inoculation, and biofilms formed on the glass tube wall as well as on the microscope slide. Following 7 days of growth, the microscope slide was removed with forceps and washed once by dipping into double-distilled water. Autofluorescence-based images were collected using a Leica SP8 confocal microscope (excitation at 630 nm and emission at 641–657 nm) [28].

For transmission electron microscopy, one day old cultures that had not yet initiated biofilm formation were sampled (10 μl) and applied onto ultra-thin carbon-coated grids. Following 5 min liquid was removed by blotting and cells were negatively stained twice with 2 % fresh aquatic uranyl acetate (10 μl) for 1 min each step. Stain was removed by blotting, grids were briefly washed with double distilled water (10 μl) and left to dry overnight at room temperature. Images were acquired with a Tecnai G2 Fei transmission electron microscope, operating at 120 kV with a 1KX1K camera [30].

3.3. Detection of YFP expressing cells by flow cytometry

Aliquots of 0.5 ml were taken from each culture tube following 2, 4 and 6 days of growth and then, in case of biofilm-forming strains, planktonic cells were removed. 1.5 ml BG11 were used to resuspend the biofilmed cells by rigorous pipetting and 0.13 ml were transferred to a 1.5 ml Eppendorf tube for homogenization with a pellet pestle (Sigma-Aldrich, Z359971-1 EA). The homogenized samples were filtered through a mesh (pore size 52 μm), supplemented with formaldehyde to a final concentration of 1 %, diluted with phosphate-buffered saline (PBS) to OD750 of ~0.0001 and measured using BD FACSAria (excitation 488 nm, emission 530 ± 30 nm). Gating for flow cytometry analysis was based on cyanobacterial autofluorescence (Fig. S6A).

3.4. Exoproteome analysis

Harvesting of CM and MS analyses were performed as described [28]. Briefly, for collection of CM, cultures were centrifuged (5000×*g* for 10 min) at room temperature, and the supernatant was removed and passed through a 0.22 μm filter. Data were analyzed to identify proteins that are significantly more or less abundant in a particular mutant's exoproteome than in the WT (false discovery rate (FDR) ≤0.1), with a cutoff of at least a 2-fold change.

3.5. RNA extraction and transcriptome analysis

Cultures of 50 ml (four biological repeats) were grown under bubbling and RNA extraction was performed 1 and 4 days after inoculation. For 4-days old *pilB*::Tn5 and *sigF1*::Mu cultures, supernatant fraction was carefully removed, and the biofilm fraction was resuspended in 3 ml of remaining supernatant. Total RNA was extracted as described [21]. Total RNA (40 μg) was treated with 4 U of TURBO™ DNase (Ambion, Catalog #: AM2238) at room temperature for 45 min followed by a boost with 4 U and an additional 45 min incubation. The DNase was removed by phenol-chloroform and chloroform extractions, RNA was precipitated and re-treated with DNAse as described above. RNA sample pellets resulting from the ethanol precipitation were washed with ice cold 70 % ethanol, air-dried and resuspended in RNase-free water. Depletion of rRNA, library construction and sequencing were performed at the NGS unit, Kanbar core facility center at Bar-Ilan University as follows. 5 μg of RNA from each sample was depleted of ribosomal RNA using the RiboMinus™ Pan-Prokaryote Probe Mix, Invitrogen™ (Bacteria 2.0, revision A.0 A46920). In the last step each sample was resuspended in 45 μl ultrapure water. RNA quality control was performed using 1 % agarose gel electrophoresis and The Agilent TapeStation system. rRNA-depleted RNA (10 μl) served for library construction using KAPA mRNA HYPER-PREP (KK8581) according to manufacturer's protocol, with a 7-cycle PCR (Kapa, Roche). The samples were pooled and sequenced on Illumina's NextSeq500, with a NextSeq 500/550 High Output Kit v2.5 (75 cycles) 20024906, resulting in total of 520 M reads. Sequenced reads were mapped to the *S. elongatus* PCC 7942 reference genome using Rockhopper [52–54]. Normalization and differentially expressed gene test were implemented by DESeq2. An arbitrary cutoff of at least 1 log2-fold and p-value adjusted for multiple testing <0.05 were chosen to define DEGs.

Raw data were deposited to the Gene Expression Omnibus GEO database (accession GSE254350).

CRediT authorship contribution statement

Shiran Suban: Writing – review & editing, Writing – original draft, Visualization, Validation, Methodology, Investigation, Formal analysis, Data curation, Conceptualization. **Sapir Yemini:** Writing – review & editing, Validation, Investigation, Formal analysis. **Anna Shor:** Writing – review & editing, Investigation, Formal analysis, Data curation. **Hiba Waldman Ben-Asher:** Writing – review & editing, Formal analysis, Data curation. **Orly Yaron:** Writing – review & editing, Methodology. **Sarit Karako-Lampert:** Writing – review & editing, Methodology. **Eleonora Sendersky:** Writing – review & editing, Visualization, Validation, Project administration, Formal analysis, Data curation, Conceptualization. **Susan S. Golden:** Writing – review & editing, Funding acquisition, Conceptualization. **Rakefet Schwarz:** Writing – review & editing, Writing – original draft, Supervision, Project administration, Investigation, Funding acquisition, Conceptualization.

Declaration of competing interest

The authors declare that they have no known competing financial interests or personal relationships that could have appeared to influence the work reported in this paper.

Data availability

Transcriptome (Original data) (Gene Expression Omnibus (GEO))

Acknowledgments

Studies in the laboratories of Rakefet Schwarz and Susan Golden were supported by the program of the National Science Foundation and

the US-Israel Binational Science Foundation (NSF-BSF 2012823). This study was also supported by a grant from the Israel Science Foundation (ISF 2494/19) to Rakefet Schwarz.

Appendix A. Supplementary data

Supplementary data to this article can be found online at https://doi.org/10.1016/j.bioflm.2024.100217.

References

[1] Srivastava A, Summers ML, Sobotka R. Cyanobacterial sigma factors: current and future applications for biotechnological advances. Biotechnol Adv 2020;40.
[2] Gruber TM, Gross CA. Multiple sigma subunits and the partitioning of bacterial transcription space. Annu Rev Microbiol 2003;57:441–66.
[3] Feklistov A, Sharon BD, Darst SA, Gross CA. Bacterial sigma factors: a historical, structural, and genomic perspective. Annu Rev Microbiol 2014;68:357–76.
[4] Helmann JD. Where to begin? Sigma factors and the selectivity of transcription initiation in bacteria. Mol Microbiol 2019;112(2):335–47.
[5] Paget MS. Bacterial sigma factors and anti-sigma factors: structure, function and distribution. Biomolecules 2015;5(3):1245–65.
[6] Wosten MM. Eubacterial sigma-factors. FEMS Microbiol Rev 1998;22(3):127–50.
[7] Lonetto MA, Donohue TJ, Gross CA, Buttner MJ. Discovery of the extracytoplasmic function sigma factors. Mol Microbiol 2019;112(2):348–55.
[8] Imamura S, Yoshihara S, Nakano S, Shiozaki N, Yamada A, Tanaka K, Takahashi H, Asayama M, Shirai M. Purification, characterization, and gene expression of all sigma factors of RNA polymerase in a cyanobacterium. J Mol Biol 2003;325(5):857–72.
[9] Imamura S, Asayama M. Sigma factors for cyanobacterial transcription. Gene Regul Syst Biol 2009;3:65–87.
[10] Rachedi R, Foglino M, Latifi A. Stress signaling in cyanobacteria: a mechanistic overview. Life 2020;10(12).
[11] Osanai T, Ikeuchi M, Tanaka K. Group 2 sigma factors in cyanobacteria. Physiol Plantarum 2008;133(3):490–506.
[12] Stensjo K, Vavitsas K, Tyystjarvi T. Harnessing transcription for bioproduction in cyanobacteria. Physiol Plantarum 2018;162(2):148–55.
[13] Gonzalez A, Riley KW, Harwood TV, Zuniga EG, Risser DD, Tripartite A. Hierarchical sigma factor cascade promotes hormogonium development in the filamentous cyanobacterium Nostoc punctiforme. mSphere 2019;4(3).
[14] Aldea MR, Mella-Herrera RA, Golden JW. Sigma factor genes sigC, sigE, and sigG are upregulated in heterocysts of the cyanobacterium Anabaena sp. strain PCC 7120. J Bacteriol 2007;189(22):8392–6.
[15] Inoue-Sakamoto K, Gruber TM, Christensen SK, Arima H, Sakamoto T, Bryant DA. Group 3 sigma factors in the marine cyanobacterium Synechococcus sp. strain PCC 7002 are required for growth at low temperature. J Gen Appl Microbiol 2007;53(2):89–104.
[16] Huckauf J, Nomura C, Forchhammer K, Hagemann M. *Stress responses of Synechocystis sp. strain PCC 6803 mutants impaired in genes encoding putative alternative sigma factors* Microbiology 2000;146(Pt 11):2877–89.
[17] Bhaya D, Watanabe N, Ogawa T, Grossman AR. The role of an alternative sigma factor in motility and pilus formation in the cyanobacterium Synechocystis sp. strain PCC6803. Proc. Nat. Acad. Sci. USA 1999;96(6):3188–93.
[18] Conradi FD, Mullineaux CW, Wilde A. The role of the cyanobacterial type IV pilus machinery in finding and maintaining a favourable environment. Life 2020;10(11).
[19] Asayama M, Imamura S. Stringent promoter recognition and autoregulation by the group 3 sigma-factor SigF in the cyanobacterium Synechocystis sp. strain PCC 6803. Nucleic Acids Res 2008;36(16):5297–305.
[20] Flores C, Santos M, Pereira SB, Mota R, Rossi F, De Philippis R, Couto N, Karunakaran E, Wright PC, Oliveira P, Tamagnini P. The alternative sigma factor SigF is a key player in the control of secretion mechanisms in Synechocystis sp. PCC 6803. Environ Microbiol 2019;21(1):343–59.
[21] Simkovsky R, Parnasa R, Wang J, Nagar E, Zecharia E, Suban S, Yegorov Y, Veltman B, Sendersky E, Schwarz R, Golden SS. Transcriptomic and phenomic investigations reveal elements in biofilm repression and formation in the cyanobacterium Synechococcus elongatus PCC 7942. Front Microbiol 2022;13:899150.
[22] Schatz D, Nagar E, Sendersky E, Parnasa R, Zilberman S, Carmeli S, Mastai Y, Shimoni E, Klein E, Yeger O, Reich Z, Schwarz R. Self-suppression of biofilm formation in the cyanobacterium Synechococcus elongatus. Environ Microbiol 2013;15(6):1786–94.
[23] Nagar E, Schwarz R. To be or not to be planktonic? Self-inhibition of biofilm development. Environ Microbiol 2015;17(5):1477–86.
[24] Parnasa R, Nagar E, Sendersky E, Reich Z, Simkovsky R, Golden S, Schwarz R. Small secreted proteins enable biofilm development in the cyanobacterium Synechococcus elongatus. Sci Rep 2016;6:32209.
[25] Frenkel A, Zecharia E, Gomez-Perez D, Sendersky E, Yegorov Y, Jacob A, Benichou JIC, Stierhof YD, Parnasa R, Golden SS, Kemen E, Schwarz R. Cell specialization in cyanobacterial biofilm development revealed by expression of a cell-surface and extracellular matrix protein. NPJ Biofilms Microbiomes 2023;9(1):10.
[26] Parnasa R, Sendersky E, Simkovsky R, Waldman Ben-Asher H, Golden SS, Schwarz R. A microcin processing peptidase-like protein of the cyanobacterium Synechococcus elongatus is essential for secretion of biofilm-promoting proteins. Environ Microbiol Rep 2019;11(3):456–63.
[27] Nagar E, Zilberman S, Sendersky E, Simkovsky R, Shimoni E, Gershtein D, Herzberg M, Golden SS, Schwarz R. Type 4 pili are dispensable for biofilm development in the cyanobacterium Synechococcus elongatus. Environ Microbiol 2017;19(7):2862–72.
[28] Yegorov Y, Sendersky E, Zilberman S, Nagar E, Waldman Ben-Asher H, Shimoni E, Simkovsky R, Golden SS, LiWang A, Schwarz R. A cyanobacterial component required for pilus biogenesis affects the exoproteome. mBio 2021;12(2).
[29] Schuergers N, Ruppert U, Watanabe S, Nurnberg DJ, Lochnit G, Dienst D, Mullineaux CW, Wilde A. Binding of the RNA chaperone Hfq to the type IV pilus base is crucial for its function in Synechocystis sp. PCC 6803. Mol Microbiol 2014;92(4):840–52.
[30] Suban S, Sendersky E, Golden SS, Schwarz R. Impairment of a cyanobacterial glycosyltransferase that modifies a pilin results in biofilm development. Environ Microbiol Rep 2022;14(2):218–29.
[31] Sendersky E, Simkovsky R, Golden S S, Schwarz R. Quantification of chlorophyll as a proxy for biofilm formation in the cyanobacterium Synechococcus elongatus. Bio-protocol 2017;7(14). https://doi.org/10.21769/BioProtoc.2406. bio-protocol.org/e2406.
[32] Taton A, Erikson C, Yang Y, Rubin BE, Rifkin SA, Golden JW, Golden SS. The circadian clock and darkness control natural competence in cyanobacteria. Nat Commun 2020;11(1):1688.
[33] Srivastava A, Brilisauer K, Rai AK, Ballal A, Forchhammer K, Tripathi AK. Down-regulation of the alternative sigma factor SigJ confers a photoprotective phenotype to Anabaena PCC 7120. Plant Cell Physiol 2017;58(2):287–97.
[34] Wetmore KM, Price MN, Waters RJ, Lamson JS, He J, Hoover CA, Blow MJ, Bristow J, Butland G, Arkin AP, Deutschbauer A. Rapid quantification of mutant fitness in diverse bacteria by sequencing randomly bar-coded transposons. mBio 2015;6(3):e00306–15.
[35] Price MN, Wetmore KM, Waters RJ, Callaghan M, Ray J, Liu H, Kuehl JV, Melnyk RA, Lamson JS, Suh Y, Carlson HK, Esquivel Z, Sadeeshkumar H, Chakraborty R, Zane GM, Rubin BE, Wall JD, Visel A, Bristow J, Blow MJ, Arkin AP, Deutschbauer AM. Mutant phenotypes for thousands of bacterial genes of unknown function. Nature 2018;557(7706):503–9.
[36] Osanai T, Imashimizu M, Seki A, Sato S, Tabata S, Imamura S, Asayama M, Ikeuchi M, Tanaka K. ChlH, the H subunit of the Mg-chelatase, is an anti-sigma factor for SigE in Synechocystis sp. PCC 6803. Proc Natl Acad Sci U S A 2009;106(16):6860–5.
[37] Bell N, Lee JJ, Summers ML. Characterization and in vivo regulon determination of an ECF sigma factor and its cognate anti-sigma factor in Nostoc punctiforme. Mol Microbiol 2017;104(1):179–94.
[38] Zhao HT, Lee J, Chen J. The hemolysin A secretion system is a multi-engine pump containing three ABC transporters. Cell 2022;185(18):3329.
[39] Linhartova M, Bucinska L, Halada P, Jecmen T, Setlik J, Komenda J, Sobotka R. Accumulation of the Type IV prepilin triggers degradation of SecY and YidC and inhibits synthesis of Photosystem II proteins in the cyanobacterium Synechocystis PCC 6803. Mol Microbiol 2014;93(6):1207–23.
[40] Bhaya D, Bianco NR, Bryant D, Grossman A. Type IV pilus biogenesis and motility in the cyanobacterium Synechocystis sp. PCC6803. Mol Microbiol 2000;37(4):941–51.
[41] Craig L, Forest KT, Maier B. Type IV pili: dynamics, biophysics and functional consequences. Nat Rev Microbiol 2019;17(7):429–40.
[42] Wallden K, Rivera-Calzada A, Waksman G. Type IV secretion systems: versatility and diversity in function. Cell Microbiol 2010;12(9):1203–12.
[43] McCallum M, Burrows LL, Howell PL. The dynamic structures of the type IV pilus. Microbiol Spectr 2019;7(2).
[44] Giltner CL, Nguyen Y, Burrows LL. Type IV pilin proteins: versatile molecular modules. Microbiol Mol Biol Rev 2012;76(4):740–72.
[45] Schuergers N, Wilde A. Appendages of the cyanobacterial cell. Life 2015;5(1):700–15.
[46] Fong JNC, Yildiz FH. Biofilm matrix proteins. Microbiol Spectr 2015;3(2).
[47] Taglialegna A, Lasa I, Valle J. Amyloid structures as biofilm matrix scaffolds. J Bacteriol 2016;198(19):2579–88.
[48] Erskine E, MacPhee CE, Stanley-Wall NR. Functional amyloid and other protein fibers in the biofilm matrix. J Mol Biol 2018;430(20):3642–56.
[49] Gomez-Perez D, Chaudhry V, Kemen A, Kemen E. Amyloid proteins in plant-associated microbial communities. Microb Physiol 2021;31(2):88–98.
[50] Merritt JH, Kadouri DE, O'Toole GA. Growing and analyzing static biofilms. Curr Protoc Microbiol 2005;1:Unit 1B 1. **Chapter**.
[51] Golden SS, Brusslan J, Haselkorn R. Genetic engineering of the cyanobacterial chromosome. Methods Enzymol 1987;153:215–31.
[52] Tjaden B. A computational system for identifying operons based on RNA-seq data. Methods 2020;176:62–70.
[53] Tjaden B. De novo assembly of bacterial transcriptomes from RNA-seq data. Genome Biol 2015;16(1):1.
[54] McClure R, Balasubramanian D, Sun Y, Bobrovskyy M, Sumby P, Genco CA, Vanderpool CK, Tjaden B. Computational analysis of bacterial RNA-Seq data. Nucleic Acids Res 2013;41(14):e140.